

DESY 96-178
October 1996

STOP DECAYS IN SUSY-QCD*

W. BEENAKKER^{1§}, R. HÖPKER², T. PLEHN² AND P. M. ZERWAS²

¹ Instituut-Lorentz, P.O. Box 9506, NL-2300 RA Leiden, The Netherlands

² Deutsches Elektronen-Synchrotron DESY, D-22603 Hamburg, FRG

Abstract

The partial widths are determined for stop decays to top quarks and gluinos, and gluino decays to stop particles and top quarks (depending on the masses of the particles involved). The widths are calculated including one-loop SUSY-QCD corrections. The radiative corrections for these strong-interaction decays are compared with the SUSY-QCD corrections for electroweak stop decays to quarks and neutralinos/charginos and top-quark decays to stops and neutralinos.

*partially supported by EU contract CHRX-CT-92-0004

§Fellow of the Royal Dutch Academy of Arts and Sciences

1 Introduction

The top and stop particles form a complex system in supersymmetric theories. The strong Yukawa coupling between top/stop and Higgs fields gives rise to a large mixing of the L and R stop states \tilde{t}_L and \tilde{t}_R , which are associated with the left and right chiral top-quark states. The mass splitting between the stop mass eigenstates \tilde{t}_1 and \tilde{t}_2 can therefore be quite large. In fact, it is possible that the mass $m_{\tilde{t}_1}$ of the lightest stop state is even smaller than the top mass m_t itself [1].

Depending on the mass values of the particles involved, quite different decay scenarios will be realized in the stop-top sector. If stop particles are very heavy, they can decay into top quarks and gluinos,

$$\tilde{t}_j \rightarrow t + \tilde{g} \quad \left[m_{\tilde{t}_j} > m_t + m_{\tilde{g}} \right] \quad (1)$$

In this paper we generalize the analysis of Ref.[2], in which the decay widths for the squarks related to the light quark species ($\tilde{q} = \tilde{u}, \dots, \tilde{b}$) were calculated, to the stop-decay processes (1) in next-to-leading order SUSY-QCD; in this more complex case the stop mixing and the non-zero top-quark mass in the final state must be taken into account. In a similar way we analyze the crossed channel

$$\tilde{g} \rightarrow \bar{t} + \tilde{t}_j \quad \text{and c.c.} \quad \left[m_{\tilde{g}} > m_t + m_{\tilde{t}_j} \right] \quad (2)$$

in leading and next-to-leading order. For small stop masses, in particular for \tilde{t}_1 , the decay channel (1) is presumably shut kinematically and decays to quarks and light neutralinos or charginos ($\tilde{t}_1 \rightarrow t\tilde{\chi}_1^0, b\tilde{\chi}_1^+$) will be dominant [3].¹ For the sake of comparison with Refs.[3, 5], we re-analyze also these decay modes in next-to-leading order SUSY-QCD. Finally, in the exceptional case $m_t > m_{\tilde{t}_1}$, the interesting decay mode $t \rightarrow \tilde{t}_1\tilde{\chi}_1^0$ may occur, see e.g. Ref.[6]; the partial width of this non-standard top decay has recently been determined in next-to-leading order SUSY-QCD in Ref.[7].

2 Theoretical Set-up

To lowest order the partial widths for the stop and gluino decays (1) and (2) are given by²

$$\Gamma(\tilde{t}_{1,2} \rightarrow t \tilde{g}) = \frac{2\alpha_s \kappa}{3m_{\tilde{t}_{1,2}}^3} \left[m_{\tilde{t}_{1,2}}^2 - m_t^2 - m_{\tilde{g}}^2 \pm 2m_t m_{\tilde{g}} \sin(2\tilde{\theta}) \right] \quad (3)$$

$$\Gamma(\tilde{g} \rightarrow \bar{t} \tilde{t}_{1,2}) = -\frac{\alpha_s \kappa}{8m_{\tilde{g}}^3} \left[m_{\tilde{t}_{1,2}}^2 - m_t^2 - m_{\tilde{g}}^2 \pm 2m_t m_{\tilde{g}} \sin(2\tilde{\theta}) \right] \quad (4)$$

¹For higher-order electroweak stop decays we refer to the recent paper Ref.[4].

² As usual, $\kappa = (\sum_i m_i^4 - \sum_{i \neq j} m_i^2 m_j^2)^{1/2}$, the sums running over all particles involved in the decay process.

Here $m_{\tilde{t}_1}$ and $m_{\tilde{t}_2}$ are the eigenvalues of the stop mass matrix³ [1, 8]:

$$\begin{aligned}\mathcal{M}^2 &= \begin{pmatrix} \mathcal{M}_{LL}^2 & \mathcal{M}_{LR}^2 \\ \mathcal{M}_{RL}^2 & \mathcal{M}_{RR}^2 \end{pmatrix} \\ &= \begin{pmatrix} m_Q^2 + m_t^2 + \left(\frac{1}{2} - \frac{2}{3}s_w^2\right)m_Z^2 \cos(2\beta) & -m_t(A_t + \mu \cot \beta) \\ -m_t(A_t + \mu \cot \beta) & m_U^2 + m_t^2 + \frac{2}{3}s_w^2 m_Z^2 \cos(2\beta) \end{pmatrix}\end{aligned}\quad (5)$$

The quantities m_Q, m_U, μ , and A_t are the usual soft SUSY-breaking mass and trilinear parameters, m_Z and s_w are the Z -boson mass and the weak mixing angle, and $\tan \beta$ is the ratio of the two vacuum expectation values in the Higgs sector. The diagonal entries of the stop mass matrix correspond to the L and R squark-mass terms, the off-diagonal entries are due to chirality-flip Yukawa interactions. The chiral states \tilde{t}_L and \tilde{t}_R are rotated into the mass eigenstates \tilde{t}_{10} and \tilde{t}_{20}

$$\begin{pmatrix} \tilde{t}_{10} \\ \tilde{t}_{20} \end{pmatrix} = \begin{pmatrix} \cos \tilde{\theta}_0 & \sin \tilde{\theta}_0 \\ -\sin \tilde{\theta}_0 & \cos \tilde{\theta}_0 \end{pmatrix} \begin{pmatrix} \tilde{t}_L \\ \tilde{t}_R \end{pmatrix}\quad (6)$$

by these Yukawa interactions. The mass eigenvalues and the rotation angle can be calculated from the mass matrix (5):

$$m_{\tilde{t}_{10}}^2, m_{\tilde{t}_{20}}^2 = \frac{1}{2} \left[\mathcal{M}_{LL}^2 + \mathcal{M}_{RR}^2 \mp [(\mathcal{M}_{LL}^2 - \mathcal{M}_{RR}^2)^2 + 4(\mathcal{M}_{LR}^2)^2]^{1/2} \right]\quad (7)$$

$$\sin(2\tilde{\theta}_0) = \frac{2\mathcal{M}_{LR}^2}{m_{\tilde{t}_{10}}^2 - m_{\tilde{t}_{20}}^2} \quad \text{and} \quad \cos(2\tilde{\theta}_0) = \frac{\mathcal{M}_{LL}^2 - \mathcal{M}_{RR}^2}{m_{\tilde{t}_{10}}^2 - m_{\tilde{t}_{20}}^2}\quad (8)$$

By definition we take \tilde{t}_{10} to correspond to the lightest stop state.

The mixing angle is an observable quantity, as evident from the decay widths (3) and (4). Since the widths of supersymmetric particles are notoriously difficult to measure, production processes may instead be adopted for the operational definition of the mixing angle in practice. Pair production in e^+e^- collisions, $e^+e^- \rightarrow \tilde{t}_i \tilde{t}_j^*$, lends itself as a convenient observable [11].

SUSY-QCD corrections, as exemplified by the diagrams of Fig.1(a), modify the stop mass matrix and the fields, necessitating the renormalization of the masses $m_{\tilde{t}_{j0}}^2 = m_{\tilde{t}_j}^2 + \delta m_{\tilde{t}_j}^2$ and of the wave functions $\tilde{t}_{i0} = Z_{ij}^{1/2} \tilde{t}_j$; the renormalization of the mixing angle can be related to the renormalization matrix $Z^{1/2}$. Without loss of generality, we may assume $Z_{12}^{1/2} = -Z_{21}^{1/2}$ since, as will be shown later, the reduced self-energy matrix $\Sigma_{ij}/(m_{\tilde{t}_i}^2 - m_{\tilde{t}_j}^2)$ is antisymmetric. In that case the renormalization matrix $Z^{1/2}$ can be written to order α_s as the product of a diagonal matrix with the elements $Z_{jj}^{1/2} = 1 + \delta Z_{jj}/2$ and a rotation matrix parametrized by the small angle $\delta\tilde{\theta}$:

$$Z^{1/2} \mapsto \begin{pmatrix} 1 + \delta Z_{11}/2 & 0 \\ 0 & 1 + \delta Z_{22}/2 \end{pmatrix} \begin{pmatrix} \cos \delta\tilde{\theta} & \sin \delta\tilde{\theta} \\ -\sin \delta\tilde{\theta} & \cos \delta\tilde{\theta} \end{pmatrix}\quad (9)$$

³ The sign conventions follow the SPYTHIA program [9], which is based on Ref.[10].

with $\delta\tilde{\theta} = Z_{12}^{1/2} = -Z_{21}^{1/2}$. Within this formalism the rotational part of $Z^{1/2}$ can be interpreted as a shift in the mixing angle, $\tilde{\theta}_0 \mapsto \tilde{\theta}_0 - \delta\tilde{\theta} \equiv \tilde{\theta}$. The remaining renormalization constants are fixed by imposing the following two conditions:

(i) The real part of the diagonal elements in the stop propagator matrix $\Delta_{ij}(p^2)$ develops poles for $p^2 \rightarrow m_{\tilde{t}_j}^2$, with the residues being unity. This requirement fixes the counterterms $\delta m_{\tilde{t}_j}^2$ and the diagonal wave-function renormalization δZ_{jj} . The so-defined renormalized stop masses $m_{\tilde{t}_j}^2$ are called pole masses.

(ii) We define a running mixing angle $\tilde{\theta}(Q^2)$ by requiring that the real part of the off-diagonal elements of the propagator matrix $\Delta_{ij}(p^2)$ vanishes for a specific value $p^2 = Q^2$ of the four-momentum squared. In this scheme the [real or virtual] particles \tilde{t}_1 and \tilde{t}_2 propagate independently of each other at four-momentum squared Q^2 and do not oscillate.

The dependence of the renormalized mixing angle $\tilde{\theta}$ on the renormalization scale Q is indicated by the notation $\tilde{\theta}(Q^2)$. Different choices for Q^2 are connected by a finite shift in $\tilde{\theta}(Q^2)$, which is calculated in the next paragraph. Quite often the renormalized mixing angle is defined in an 'on-shell renormalization scheme' [5, 12] in which the renormalization of the mixing angle cannot be linked to the stop wave functions any more. Even though the definitions of the mixing angle are different in the two schemes, the physical observables, widths and cross-sections are of course equivalent to $\mathcal{O}(\alpha_s)$.

In carrying out this renormalization program we find the following expressions for the various counter terms:

$$\delta m_{\tilde{t}_j}^2 = \text{Re } \Sigma_{jj}(m_{\tilde{t}_j}^2) \quad \delta Z_{jj} = -\text{Re } \dot{\Sigma}_{jj}(m_{\tilde{t}_j}^2) \quad \delta\tilde{\theta} = -\text{Re } \Sigma_{12}(Q^2)/[m_{\tilde{t}_2}^2 - m_{\tilde{t}_1}^2]$$

Here $\Sigma_{ij}(p^2)$ and $\dot{\Sigma}_{ij}(p^2) = \partial \Sigma_{ij}(p^2)/\partial p^2$ denote the unrenormalized self-energy matrix and its derivative [see also Ref. [12, 5]] :

$$\Sigma_{12}(p^2) = -2\pi C_F \alpha_s \left\{ s_{4\tilde{\theta}} \left[A(m_{\tilde{t}_2}) - A(m_{\tilde{t}_1}) \right] + 8m_{\tilde{g}}m_t c_{2\tilde{\theta}} B(p^2, m_{\tilde{g}}, m_t) \right\} \quad (10)$$

$$\Sigma_{21}(p^2) = \Sigma_{12}(p^2) \quad (11)$$

$$\begin{aligned} \Sigma_{11}(p^2) = -4\pi C_F \alpha_s \left\{ (1 + c_{2\tilde{\theta}}^2) A(m_{\tilde{t}_1}) + s_{2\tilde{\theta}}^2 A(m_{\tilde{t}_2}) \right. \\ \left. - 2 A(m_{\tilde{g}}) - 2 A(m_t) - 2 (p^2 + m_{\tilde{t}_1}^2) B(p^2, \lambda, m_{\tilde{t}_1}) \right. \\ \left. + 2 (p^2 - m_{\tilde{g}}^2 - m_t^2 + 2m_{\tilde{g}}m_t s_{2\tilde{\theta}}) B(p^2, m_{\tilde{g}}, m_t) \right\} \quad (12) \end{aligned}$$

$$\begin{aligned} \Sigma_{22}(p^2) = -4\pi C_F \alpha_s \left\{ (1 + c_{2\tilde{\theta}}^2) A(m_{\tilde{t}_2}) + s_{2\tilde{\theta}}^2 A(m_{\tilde{t}_1}) \right. \\ \left. - 2 A(m_{\tilde{g}}) - 2 A(m_t) - 2 (p^2 + m_{\tilde{t}_2}^2) B(p^2, \lambda, m_{\tilde{t}_2}) \right. \\ \left. + 2 (p^2 - m_{\tilde{g}}^2 - m_t^2 - 2m_{\tilde{g}}m_t s_{2\tilde{\theta}}) B(p^2, m_{\tilde{g}}, m_t) \right\} \quad (13) \end{aligned}$$

[We have used the standard notation $s_\theta \equiv \sin \theta$ etc.] The first two terms in $\Sigma_{12}(p^2)$, involving the p^2 -independent 1-point function A , follow from the third Feynman diagram in Fig.1(a), the remaining term given by the 2-point function B , corresponds to the second diagram in Fig.1(a). As both A and B are ultraviolet (UV) divergent⁴, also $\delta\tilde{\theta}$ is UV divergent; in $n = 4 - 2\epsilon$ dimensions:

$$\delta\tilde{\theta} |_{div} = \frac{C_F \alpha_s}{8\pi(m_{\tilde{t}_1}^2 - m_{\tilde{t}_2}^2)} \left[s_{4\tilde{\theta}} \left(m_{\tilde{t}_2}^2 - m_{\tilde{t}_1}^2 \right) + 8m_{\tilde{g}}m_t c_{2\tilde{\theta}} \right] \frac{1}{\epsilon} \quad (14)$$

The change of the renormalized angle $\tilde{\theta}(Q^2)$ between two different values of Q^2 is finite:

$$\tilde{\theta}(Q'^2) - \tilde{\theta}(Q^2) = - \frac{16\pi C_F \alpha_s m_{\tilde{g}} m_t \cos(2\tilde{\theta})}{m_{\tilde{t}_2}^2 - m_{\tilde{t}_1}^2} \text{Re} \left[B(Q'^2, m_{\tilde{g}}, m_t) - B(Q^2, m_{\tilde{g}}, m_t) \right] \quad (15)$$

This shift is independent of the regularization scheme. For illustration the normalized shift relative to $\tilde{\theta}(m_{\tilde{t}_1}^2)$: $[\tilde{\theta}(Q^2) - \tilde{\theta}(m_{\tilde{t}_1}^2)]/\tilde{\theta}(m_{\tilde{t}_1}^2)$, is shown in Fig.2.

3 Stop and Gluino Decays

The diagrams relevant for stop and gluino decays are presented in Fig.3. This set is complemented by the self-energy diagrams for the stop particles, the gluinos, and the top quarks, displayed in Fig.1. The Born diagrams are presented in Fig.3(a) for the two decay channels, the vertex corrections in Fig.3(b), and the hard-gluon radiation in Fig.3(c). In Figs.3(b) and (c) only the stop-decay diagrams are depicted, since gluino- and stop-decay diagrams are related by crossing. The ultraviolet divergences are regularized in n dimensions, infrared and collinear divergences⁵ by introducing a small gluon mass λ . The renormalization of the strong coupling constants g_s and \hat{g}_s are carried out in the $\overline{\text{MS}}$ renormalization scheme at the charge-renormalization scale μ_R ; a finite shift [13] between the bare Yukawa coupling \hat{g}_s and the bare gauge coupling g_s restores supersymmetry at the one-loop level in the $\overline{\text{MS}}$ scheme [see Ref.[2] for explicit verification]:

$$\hat{g}_s = g_s \left[1 + \frac{\alpha_s}{8\pi} \left(\frac{4}{3} N_c - C_F \right) \right] \quad (16)$$

[Similarly the electroweak $\tilde{t}_i t \tilde{\chi}_j^0$ and $\tilde{t}_i b \tilde{\chi}_j^+$ couplings may be written as $a \hat{e} + b \hat{Y}_t + c \hat{Y}_b$, with $\hat{e} = e [1 - \alpha_s C_F / (8\pi)]$ and $\hat{Y}_q = Y_q [1 - 3\alpha_s C_F / (8\pi)]$ in terms of the electromagnetic coupling e and the quark-Higgs Yukawa coupling $Y_q \propto e m_q$.] The heavy particles (top quarks, squarks, gluinos) are removed from the μ_R^2 evolution of $\alpha_s(\mu_R^2)$, decoupled

⁴The definitions of the scalar functions A and B can be found in the Appendix.

⁵ Since no ggg three-gluon vertices are involved in the calculation, infrared singularities can be regularized by a non-zero gluon mass. This method can also be applied to SUSY-QCD processes including $g\tilde{g}\tilde{g}$ vertices of massive gluinos.

smoothly for momenta smaller than their masses. The masses of these heavy particles are defined as pole masses. In the numerical analyses we have inserted the mass of the decaying particle for the renormalization scale μ_R .

The detailed analytic results for stop and gluino decays are presented in the Appendix. In this section we illustrate the characteristic features of the results by numerical evaluation of a few typical examples, which properly reflect the size of the SUSY-QCD effects in general.

The masses and mixing parameters chosen in the examples are calculated from the universal SUGRA parameters [14]: the common scalar mass m_0 , the common gaugino mass $m_{1/2}$, the trilinear coupling A_0 , the ratio of the vacuum expectation values of the Higgs fields $\tan\beta$, and the sign of the higgsino mass parameter μ . The top-quark mass is set to $m_t = 175$ GeV, and the Higgs parameter $\tan\beta$ is fixed to 1.75. From this set, the pole masses of the charginos, neutralinos, gluinos, and squarks, as well as the squark mixing matrices can be calculated. We use the approximate formulae implemented in SPYTHIA [9]. We define a degenerate squark mass by averaging over the five non-top flavors. The renormalized stop mixing angle $\tilde{\theta}(m_{\tilde{t}_1}^2)$ is defined in this basis by imposing the lowest-order relation Eq. (8) in terms of the renormalized (pole) masses.⁶ The mixing angles at other renormalization scales can be obtained by adding the appropriate finite shifts [see Eq.(15)].

(a) $\tilde{t}_2 \rightarrow t + \tilde{g}$

for $m_0 = 800$ GeV, $A_0 = 200$ GeV, $\mu > 0$

In Fig.4(a) the stop and gluino masses are given as a function of the common gaugino mass $m_{1/2}$. For the indicated set of parameters the decay $\tilde{t}_2 \rightarrow t\tilde{g}$ is the only strong-interaction decay mode that is kinematically allowed.

In Fig.4(b) the width of \tilde{t}_2 is presented in lowest order and in next-to-leading order as a function of $m_{\tilde{t}_2}$. Since in this example $m_{\tilde{g}}$ rises faster than $m_{\tilde{t}_2}$ with increasing $m_{1/2}$, the width drops to zero when $m_{\tilde{t}_2}$ is increased. The radiative SUSY-QCD corrections vary between +35%, at the lower end of the spectrum, and $\sim +100\%$ at the upper end of the spectrum, *i.e.*, the corrections are large and positive.

(b) $\tilde{g} \rightarrow \tilde{t}_1 \bar{t} + \tilde{t}_1 t$

for $m_0 = 400$ GeV, $A_0 = 200$ GeV, $\mu > 0$

In a form analogous to the preceding example, masses and widths are displayed in Figs.5(a) and (b). Since $m_{\tilde{g}}$ rises faster than $m_{\tilde{t}_1}$, the width increases with increasing gluino mass. However, in contrast to stop decays, the SUSY-QCD corrections to gluino decays are only modest and negative [$\sim -10\%$]. This result is familiar from the analysis in Ref.[2], where it had been demonstrated analytically that negative π^2 terms, arising from the crossing

⁶Equivalently the mass-matrix parameters m_Q , m_U , and A_t may be chosen as basic parameters, and $\tilde{\theta}(m_{\tilde{t}_1}^2)$ and $m_{\tilde{t}_j}$ may subsequently be defined in this basis by imposing the lowest-order relations Eqs. (7) and (8). We have checked that the two schemes are equivalent.

of diagrams, give rise to destructive interference effects such that the overall correction is small.

$$(c) \quad \tilde{t}_1 \rightarrow t + \tilde{\chi}_j^0 \quad [j = 1, \dots] \quad \text{and} \quad \tilde{t}_1 \rightarrow b + \tilde{\chi}_j^+ \quad [j = 1, 2]$$

for $m_0 = 50 \text{ GeV}$, $A_0 = 100 \text{ GeV}$, $\mu < 0$

For the sake of comparison we have re-analyzed stop decays into neutralinos and charginos. The results agree with the analysis in Ref.[3], and also with the parallel calculation in Ref.[5], with which detailed point-by-point comparisons have been performed. For the set of parameters chosen in the figures, only two neutralino decay modes are kinematically allowed. The SUSY-QCD corrections to the decays into neutralinos are small [Fig.6(b)], typically less than 10%. The picture is quite similar for the decays into charginos [Fig.7(b)], though the corrections are slightly larger as a result of the massless b quarks in the final state.

$$(d) \quad t \rightarrow \tilde{t}_1 + \tilde{\chi}_j^0 \quad [j = 1, \dots]$$

for $m_0 = 250 \text{ GeV}$, $A_0 = 800 \text{ GeV}$, $\mu > 0$

As in the previous case (c), this last example is shown merely as a cross-check with Ref.[7]. As shown in Fig.8(b), the corrections are small. If this top-decay mode is realized in nature, the branching ratio for decays into $\tilde{\chi}_1^0$ can in principle be of the order of 4%. [Note that $\Gamma(t \rightarrow bW^+) \simeq 1.4 \text{ GeV}$ for $m_t = 175 \text{ GeV}$ [15]].

Since the $\tilde{t}_j/\tilde{g}/t$ SUSY decay modes could only be illustrated for a specific set of parameters, a general program⁷ has been constructed for generating all relevant decay widths in the stop-top sector.

4 Summary

In this paper we have analyzed the SUSY-QCD corrections for stop decays to top quarks and gluinos, and gluino decays to stop particles and top quarks. In contrast to earlier analyses, the non-zero top-quark mass must be taken into account in these decay modes. Moreover, the L/R squark mixing plays an important role.

We have set up a scheme in which the mixing angle $\tilde{\theta}(Q^2)$ is defined in such a way that the virtual/real stop particles \tilde{t}_1 and \tilde{t}_2 do not oscillate for a specific value of the four-momentum squared Q^2 . Convenient choices for Q^2 are $Q^2 = m_{\tilde{t}_1}^2$ or $m_{\tilde{t}_2}^2$, depending on the problem treated in the analysis. Different conventions are connected by simple relations between the associated mixing angles.

As observed earlier for squarks related to the light quark species, the SUSY-QCD corrections are large and positive for stop decays to top quarks and gluinos. They are modest and negative for gluino decays to stop particles and top quarks. We have compared

⁷The FORTRAN program may be obtained from plehn@desy.de.

these modes with other stop-decay modes, which have been analyzed earlier [3, 5]. In contrast to the strong-interaction decays, the SUSY-QCD corrections for electroweak stop decays into neutralinos and charginos are small, and so are the corrections for top-quark decays to stop particles and the lightest neutralino.

5 Acknowledgments

We are grateful to the authors of Ref.[5], especially A. Djouadi and C. Jünger, for the mutual comparison of results on the electroweak stop decays, and for general discussions on the problems treated in this paper. We thank P. Ohmann for providing us with a program in which the renormalization-group equations are solved for the masses of supersymmetric particles in supergravity scenarios. Special thanks go also to A. Bartl, A. Djouadi and W. Majerotto for valuable comments on the manuscript.

6 Appendix

In this appendix we present the explicit formulae for the calculation of the decay width of \tilde{t}_1 particles to top quarks and gluinos in next-to-leading order SUSY-QCD. The results for the decay of \tilde{t}_2 particles can be derived by interchanging the stop masses and switching the sign in front of $\sin(2\tilde{\theta})$ and $\cos(2\tilde{\theta})$. The gluino decay width $\Gamma(\tilde{g} \rightarrow \tilde{t}\tilde{t}_j)$ can be obtained from $\Gamma(\tilde{t}_j \rightarrow t\tilde{g})$ by adding a factor $-m_{\tilde{t}_j}^3/(4C_F m_{\tilde{g}}^3)$ and subsequent analytical continuation from the region $m_{\tilde{t}_j} > m_t + m_{\tilde{g}}$ to the region $m_{\tilde{g}} > m_t + m_{\tilde{t}_j}$. The multiplicative factor reflects the difference in phase-space, in color/spin averaging, and in the sign of the gluino momentum inside the spinor sum [see also Eqs. (3) and (4)].

The decay width in next-to-leading order may be split into the following components:

$$\Gamma_{\text{NLO}} = \Gamma_{\text{LO}} + \text{Re}[\Delta\Gamma_t + \Delta\Gamma_{\tilde{g}} + \Delta\Gamma_{11} + \Delta\Gamma_v + \Delta\Gamma_r + \Delta\Gamma_c + \Delta\Gamma_f + \Delta\Gamma_{\text{dec}}]$$

To allow for more compact expressions we first define a few short-hand notations:

$$\begin{aligned}\mu_{abc} &= m_a^2 + m_b^2 - m_c^2 & \sigma_{2\tilde{\theta}} &= m_t m_{\tilde{g}} \sin(2\tilde{\theta}) \\ \mathcal{N} &= \frac{\kappa}{16\pi m_{\tilde{t}_1}^3 N_c} \\ \kappa &= \left[m_{\tilde{t}_1}^4 + m_{\tilde{g}}^4 + m_t^4 - 2(m_{\tilde{t}_1}^2 m_{\tilde{g}}^2 + m_{\tilde{t}_1}^2 m_t^2 + m_{\tilde{g}}^2 m_t^2) \right]^{1/2}\end{aligned}$$

where $abc = \tilde{g}, t, j$ with j representing \tilde{t}_j .

We list the components defined above for the next-to-leading order decay width [the $1/\varepsilon$ poles in the scalar integrals cancel against each other in the final sum]:

lowest-order decay width:

$$\Gamma_{\text{LO}} = 8N_c C_F \pi \alpha_s \left(-\mu_{\tilde{g}t1} + 2\sigma_{2\tilde{\theta}} \right) \mathcal{N} \equiv \mathcal{N} |\mathcal{M}_B|^2$$

top self-energy contribution:

$$\begin{aligned}\Delta\Gamma_t = & \frac{2C_F\mathcal{N}}{m_t^2} \pi\alpha_s |\mathcal{M}_B|^2 \left\{ 2(1-\epsilon)A(m_t) + 2A(m_{\tilde{g}}) - A(m_{\tilde{t}_1}) - A(m_{\tilde{t}_2}) \right. \\ & + \mu_{t1\tilde{g}}B(p_t^2, m_{\tilde{g}}, m_{\tilde{t}_1}) + \mu_{t2\tilde{g}}B(p_t^2, m_{\tilde{g}}, m_{\tilde{t}_2}) \\ & - 4m_t^2\sigma_{2\tilde{\theta}}[\dot{B}(p_t^2, m_{\tilde{g}}, m_{\tilde{t}_1}) - \dot{B}(p_t^2, m_{\tilde{g}}, m_{\tilde{t}_2})] \\ & \left. + 2m_t^2[\mu_{\tilde{g}t1}\dot{B}(p_t^2, m_{\tilde{g}}, m_{\tilde{t}_1}) + \mu_{\tilde{g}t2}\dot{B}(p_t^2, m_{\tilde{g}}, m_{\tilde{t}_2}) - 4m_t^2\dot{B}(p_t^2, \lambda, m_t)] \right\} \\ & + \frac{16N_cC_F^2\mathcal{N}}{m_t^2} \pi^2\alpha_s^2 c_{2\tilde{\theta}}^2 \mu_{\tilde{g}t1} \left\{ A(m_{\tilde{t}_2}) - A(m_{\tilde{t}_1}) - \mu_{\tilde{g}t1}B(p_t^2, m_{\tilde{g}}, m_{\tilde{t}_1}) + \mu_{\tilde{g}t2}B(p_t^2, m_{\tilde{g}}, m_{\tilde{t}_2}) \right\}\end{aligned}$$

gluino self-energy contribution (for $n_f = 6$ quark flavors):

$$\begin{aligned}\Delta\Gamma_{\tilde{g}} = & \frac{4\mathcal{N}}{m_{\tilde{g}}^2} \pi\alpha_s |\mathcal{M}_B|^2 (n_f - 1) \left\{ -A(m_{\tilde{q}}) + (m_{\tilde{q}}^2 + m_{\tilde{g}}^2)B(p_{\tilde{g}}^2, m_{\tilde{q}}, 0) + 2m_{\tilde{g}}^2(m_{\tilde{g}}^2 - m_{\tilde{q}}^2)\dot{B}(p_{\tilde{g}}^2, m_{\tilde{q}}, 0) \right\} \\ & + \frac{2\mathcal{N}}{m_{\tilde{g}}^2} \pi\alpha_s |\mathcal{M}_B|^2 \left\{ 2A(m_t) - A(m_{\tilde{t}_1}) - A(m_{\tilde{t}_2}) + \mu_{1\tilde{g}t}B(p_{\tilde{g}}^2, m_{\tilde{t}_1}, m_t) + \mu_{2\tilde{g}t}B(p_{\tilde{g}}^2, m_{\tilde{t}_2}, m_t) \right. \\ & - 4m_{\tilde{g}}^2\sigma_{2\tilde{\theta}}[\dot{B}(p_{\tilde{g}}^2, m_{\tilde{t}_1}, m_t) - \dot{B}(p_{\tilde{g}}^2, m_{\tilde{t}_2}, m_t)] \\ & \left. + 2m_{\tilde{g}}^2[\mu_{\tilde{g}t1}\dot{B}(p_{\tilde{g}}^2, m_{\tilde{t}_1}, m_t) + \mu_{\tilde{g}t2}\dot{B}(p_{\tilde{g}}^2, m_{\tilde{t}_2}, m_t)] \right\} \\ & + \frac{4\mathcal{N}}{m_{\tilde{g}}^2} \pi\alpha_s |\mathcal{M}_B|^2 N_c \left\{ (1-\epsilon)A(m_{\tilde{g}}) - 4m_{\tilde{g}}^4\dot{B}(p_{\tilde{g}}^2, \lambda, m_{\tilde{g}}) \right\}\end{aligned}$$

diagonal stop self-energy:

$$\begin{aligned}\Delta\Gamma_{11} = & 8C_F\mathcal{N}\pi\alpha_s |\mathcal{M}_B|^2 \left\{ B(p_{\tilde{t}_1}^2, m_{\tilde{g}}, m_t) - B(p_{\tilde{t}_1}^2, \lambda, m_{\tilde{t}_1}) + 2\sigma_{2\tilde{\theta}}\dot{B}(p_{\tilde{t}_1}^2, m_{\tilde{g}}, m_t) \right. \\ & \left. - \mu_{\tilde{g}t1}\dot{B}(p_{\tilde{t}_1}^2, m_{\tilde{g}}, m_t) - 2m_{\tilde{t}_1}^2\dot{B}(p_{\tilde{t}_1}^2, \lambda, m_{\tilde{t}_1}) \right\}\end{aligned}$$

[The off-diagonal mixing contribution

$$\Delta\Gamma_{12} = \frac{128N_cC_F^2\mathcal{N}}{m_{\tilde{t}_1}^2 - m_{\tilde{t}_2}^2} \pi^2\alpha_s^2 \sigma_{2\tilde{\theta}} c_{2\tilde{\theta}}^2 \left\{ A(m_{\tilde{t}_2}) - A(m_{\tilde{t}_1}) + \frac{4m_{\tilde{t}_1}^2 m_{\tilde{g}}^2}{\sigma_{2\tilde{\theta}}} B(p_{\tilde{t}_1}^2, m_{\tilde{g}}, m_t) \right\}$$

is absorbed into the renormalization of the mixing angle for $\tilde{\theta} = \tilde{\theta}(m_{\tilde{t}_1}^2)$.]

vertex corrections:

$$\begin{aligned}\Delta\Gamma_v = & 64\mathcal{N}\pi^2\alpha_s^2 N_c C_F^2 \left[F_1^F + \sigma_{2\tilde{\theta}}F_2^F + \sigma_{2\tilde{\theta}}^2 F_3^F \right] \\ & + 32\mathcal{N}\pi^2\alpha_s^2 N_c^2 C_F \left[F_1^A + \sigma_{2\tilde{\theta}}F_2^A + \sigma_{2\tilde{\theta}}^2 F_3^A \right] \\ & + 8\mathcal{N}\pi\alpha_s |\mathcal{M}_B|^2 F^B\end{aligned}$$

with:

$$\begin{aligned}
F_1^F &= 2(m_t^2 + m_{\tilde{g}}^2)B(p_{\tilde{t}_1}^2, m_{\tilde{g}}, m_t) + (m_{\tilde{t}_1}^2 + m_t^2 + m_{\tilde{g}}^2)B(p_{\tilde{t}_1}^2, \lambda, m_{\tilde{t}_1}) \\
&\quad + 2(m_{\tilde{g}}^2 - m_{\tilde{t}_1}^2)B(p_t^2, \lambda, m_t) - 2m_t^2 B(p_t^2, m_{\tilde{g}}, m_{\tilde{t}_2}) - 4m_{\tilde{g}}^2 B(p_{\tilde{g}}^2, m_t, m_{\tilde{t}_1}) \\
&\quad + 4m_{\tilde{g}}^2(m_{\tilde{t}_1}^2 - m_{\tilde{g}}^2)C(p_{\tilde{t}_1}, -p_t, m_t, m_{\tilde{g}}, m_{\tilde{t}_1}) + 2m_t^2(m_{\tilde{t}_1}^2 + m_{\tilde{t}_2}^2 - 2m_{\tilde{t}_1}^2)C(p_{\tilde{t}_1}, -p_t, m_t, m_{\tilde{g}}, m_{\tilde{t}_2}) \\
F_2^F &= -2B(p_{\tilde{t}_1}^2, \lambda, m_{\tilde{t}_1}) - 2B(p_t^2, \lambda, m_t) - 4B(p_{\tilde{t}_1}^2, m_{\tilde{g}}, m_t) + 2B(p_t^2, m_{\tilde{g}}, m_{\tilde{t}_1}) \\
&\quad + 4B(p_{\tilde{g}}^2, m_t, m_{\tilde{t}_1}) + 4\mu_{\tilde{g}t1}C(p_{\tilde{t}_1}, -p_t, m_t, m_{\tilde{g}}, m_{\tilde{t}_1}) + 2(m_{\tilde{t}_1}^2 - m_{\tilde{t}_2}^2)C(p_{\tilde{t}_1}, -p_t, m_t, m_{\tilde{g}}, m_{\tilde{t}_2}) \\
F_3^F &= \frac{1}{m_{\tilde{g}}^2 m_t^2} \left\{ 2m_t^2 [B(p_t^2, m_{\tilde{g}}, m_{\tilde{t}_2}) - B(p_t^2, m_{\tilde{g}}, m_{\tilde{t}_1})] + \mu_{\tilde{g}t1}(\mu_{\tilde{g}t1} - 4m_t^2)C(p_{\tilde{t}_1}, -p_t, m_t, m_{\tilde{g}}, m_{\tilde{t}_1}) \right. \\
&\quad \left. - (\mu_{\tilde{g}t1}\mu_{\tilde{g}t2} - 2m_t^2\mu_{\tilde{g}t1} - 2m_t^2\mu_{\tilde{g}t2})C(p_{\tilde{t}_1}, -p_t, m_t, m_{\tilde{g}}, m_{\tilde{t}_2}) \right\} \\
F_1^A &= -2\epsilon\mu_{\tilde{g}t1}B(p_{\tilde{t}_1}^2, m_{\tilde{g}}, m_t) + 4(m_t^2 - m_{\tilde{t}_1}^2)B(p_{\tilde{g}}^2, \lambda, m_{\tilde{g}}) \\
&\quad + 2m_t^2[B(p_t^2, m_{\tilde{g}}, m_{\tilde{t}_2}) - B(p_t^2, m_{\tilde{g}}, m_{\tilde{t}_1})] + 4m_{\tilde{g}}^2 B(p_{\tilde{g}}^2, m_t, m_{\tilde{t}_1}) \\
&\quad + 4m_{\tilde{g}}^2(m_{\tilde{g}}^2 - m_{\tilde{t}_1}^2)C(p_{\tilde{t}_1}, -p_t, m_t, m_{\tilde{g}}, m_{\tilde{t}_1}) - 2m_t^2(m_{\tilde{t}_1}^2 + m_{\tilde{t}_2}^2 - 2m_{\tilde{t}_1}^2)C(p_{\tilde{t}_1}, -p_t, m_t, m_{\tilde{g}}, m_{\tilde{t}_2}) \\
F_2^A &= 4\epsilon B(p_{\tilde{t}_1}^2, m_{\tilde{g}}, m_t) - 4B(p_{\tilde{g}}^2, \lambda, m_{\tilde{g}}) - 4B(p_{\tilde{g}}^2, m_t, m_{\tilde{t}_1}) \\
&\quad - 4\mu_{\tilde{g}t1}C(p_{\tilde{t}_1}, -p_t, m_t, m_{\tilde{g}}, m_{\tilde{t}_1}) - 2(m_{\tilde{t}_1}^2 - m_{\tilde{t}_2}^2)C(p_{\tilde{t}_1}, -p_t, m_t, m_{\tilde{g}}, m_{\tilde{t}_2}) \\
F_3^A &= \frac{1}{m_{\tilde{g}}^2 m_t^2} \left\{ 2m_t^2 [B(p_t^2, m_{\tilde{g}}, m_{\tilde{t}_1}) - B(p_t^2, m_{\tilde{g}}, m_{\tilde{t}_2})] + \mu_{\tilde{g}t1}(4m_t^2 - \mu_{\tilde{g}t1})C(p_{\tilde{t}_1}, -p_t, m_t, m_{\tilde{g}}, m_{\tilde{t}_1}) \right. \\
&\quad \left. + (\mu_{\tilde{g}t1}\mu_{\tilde{g}t2} - 2m_t^2\mu_{\tilde{g}t1} - 2m_t^2\mu_{\tilde{g}t2})C(p_{\tilde{t}_1}, -p_t, m_t, m_{\tilde{g}}, m_{\tilde{t}_2}) \right\} \\
F^B &= N_c [\mu_{t1\tilde{g}}C(p_{\tilde{t}_1}, -p_t, m_{\tilde{t}_1}, \lambda, m_t) - \mu_{\tilde{g}t1}C(p_{\tilde{t}_1}, -p_t, m_{\tilde{g}}, m_t, \lambda) - \mu_{1\tilde{g}t}C(p_{\tilde{t}_1}, -p_t, \lambda, m_{\tilde{t}_1}, m_{\tilde{g}})] \\
&\quad - 2C_F\mu_{t1\tilde{g}}C(p_{\tilde{t}_1}, -p_t, m_{\tilde{t}_1}, \lambda, m_t)
\end{aligned}$$

corrections from real-gluon radiation:

$$\begin{aligned}
\Delta\Gamma_r &= \frac{\alpha_s}{4\pi^2 m_{\tilde{t}_1}} |\mathcal{M}_B|^2 \left[(m_{\tilde{t}_1}^2 - m_t^2)I_{\tilde{t}_1\tilde{g}} - m_t^2 I_{\tilde{t}_1 t} - m_{\tilde{g}}^2 I_{\tilde{g}\tilde{g}} - I_{\tilde{g}} \right] \\
&\quad + \frac{\alpha_s C_F}{4\pi^2 m_{\tilde{t}_1} N_c} |\mathcal{M}_B|^2 \left[-m_{\tilde{t}_1}^2 I_{\tilde{t}_1\tilde{t}_1} - m_t^2 I_{tt} + \mu_{t1\tilde{g}} I_{\tilde{t}_1 t} + I_{\tilde{t}_1} - I_t \right] \\
&\quad + \frac{\alpha_s^2 C_F}{\pi m_{\tilde{t}_1}} \left[C_F I_t^{\tilde{g}} + N_c I_{\tilde{g}}^{\tilde{t}_1} \right]
\end{aligned}$$

renormalization of the coupling constant:

$$\Delta\Gamma_c = -\frac{\mathcal{N}\alpha_s}{4\pi} |\mathcal{M}_B|^2 \left[\frac{1}{\epsilon} - \gamma_E + \log(4\pi) - \log\left(\frac{\mu_R^2}{\mu^2}\right) \right] \left(\frac{11}{3}N_c - \frac{2}{3}N_c - \frac{2}{3}n_f - \frac{1}{3}n_f \right)$$

finite shift of the Yukawa coupling relative to the gauge coupling in $\overline{\text{MS}}$:

$$\Delta\Gamma_f = \frac{\mathcal{N}\alpha_s}{4\pi} |\mathcal{M}_B|^2 \left(\frac{4}{3}N_c - C_F \right)$$

decoupling of the heavy flavors from the running strong coupling:

$$\Delta\Gamma_{\text{dec}} = \frac{\mathcal{N}\alpha_s}{\pi} |\mathcal{M}_B|^2 \left\{ \frac{n_f - 1}{12} \log \left(\frac{\mu_R^2}{m_q^2} \right) + \frac{1}{24} \log \left(\frac{\mu_R^2}{m_{t_1}^2} \right) + \frac{1}{24} \log \left(\frac{\mu_R^2}{m_{t_2}^2} \right) \right. \\ \left. + \frac{1}{6} \log \left(\frac{\mu_R^2}{m_t^2} \right) + \frac{N_c}{6} \log \left(\frac{\mu_R^2}{m_{\bar{g}}^2} \right) \right\}$$

In these expressions the invariant integrals are defined as

$$I_{ab\dots}^{AB\dots} = \frac{1}{\pi^2} \int \frac{d^3 p_t}{2p_t^0} \frac{d^3 p_{\bar{g}}}{2p_{\bar{g}}^0} \frac{d^3 q}{2q^0} \delta_4 \left(q + p_t + p_{\bar{g}} - p_{t_1} \right) \frac{(2qp_A)(2qp_B) \dots}{(2qp_a)(2qp_b) \dots} \\ A(m_a) = \mu^{2\epsilon} \int \frac{d^n q}{(2\pi)^n} \frac{i}{q^2 - m_a^2} \\ B(p^2, m_a, m_b) = \mu^{2\epsilon} \int \frac{d^n q}{(2\pi)^n} \frac{i}{[q^2 - m_a^2][(q + p)^2 - m_b^2]} \\ C(p_1, p_2, m_a, m_b, m_c) = \mu^{2\epsilon} \int \frac{d^n q}{(2\pi)^n} \frac{i}{[q^2 - m_a^2][(q + p_1)^2 - m_b^2][(q + p_1 + p_2)^2 - m_c^2]} \\ \dot{B}(p^2, m_a, m_b) = \partial B(p^2, m_a, m_b) / \partial p^2$$

Note that in the angular integrals $I_{ab\dots}^{AB\dots}$ from real-gluon radiation we do not add a minus sign for every term $(2qp_{t_1})$, in contrast to Ref.[16].⁸ In the numerical analyses we have inserted the mass of the decaying particle for the renormalization scale μ_R . The scale parameter μ accounts for the correct dimension of the coupling in n dimensions, cancelled together with the $1/\epsilon$ poles.

References

- [1] J. Ellis and S. Rudaz, *Phys. Lett.* **B128** (1983) 248.
- [2] W. Beenakker, R. Höpker, and P. M. Zerwas, *Phys. Lett.* **B378** (1996) 159.
- [3] S. Kraml, H. Eberl, A. Bartl, W. Majerotto, and W. Porod, Vienna preprint UWTHPH-1996-35 (hep-ph/9605412).
- [4] W. Porod and T. Wöhrmann, Vienna preprint UWTHPH-1996-45 (hep-ph/9608472).
- [5] A. Djouadi, W. Hollik, and C. Jünger, Karlsruhe preprint KA-TP-20-96 (hep-ph/9609419).
- [6] F. Borzumati, Proceedings, e^+e^- Collisions at TeV Energies: The Physics Potential, ed. P. M. Zerwas, DESY 96-123D.

⁸It should be noted that Eqs.(D.11) and (D.12) of Ref.[16] must be corrected in the following way: The first term in the square brackets of Eq.(D.11) has to be replaced by the corresponding term in Eq.(D.12), and *vice versa*.

- [7] A. Djouadi, W. Hollik, and C. Jünger, Karlsruhe preprint KA-TP-14-96 (hep-ph/9605340).
- [8] J. F. Gunion and H. E. Haber, *Nucl. Phys.* **B272** (1986) 1.
- [9] S. Mrenna, Argonne preprint ANL-HEP-PR-96-63 (hep-ph/9609360).
- [10] M. Drees and S. P. Martin, Madison preprint MAD-PH-879 (hep-ph/9504324).
- [11] K. Hikasa and M. Kobayashi, *Phys. Rev.* **D36** (1987) 724.
- [12] H. Eberl, A. Bartl and W. Majerotto, *Nucl. Phys.* **B472** (1996) 481.
- [13] S. P. Martin and M. T. Vaughn, *Phys. Lett.* **B318** (1993) 331.
- [14] V. Barger, M. S. Berger, and P. Ohmann, *Phys. Rev.* **D47** (1993) 1093 and *Phys. Rev.* **D49** (1994) 4908; M. Carena, M. Olechowski, S. Pokorski, and C. E. M. Wagner, *Nucl. Phys.* **B419** (1994) 213.
- [15] I. I. Bigi, Y. L. Dokshitzer, V. A. Khoze, J. H. Kühn, and P. M. Zerwas, *Phys. Lett.* **B181** (1986) 157.
- [16] A. Denner, *Fortschr. Phys.* **41** (1993) 307

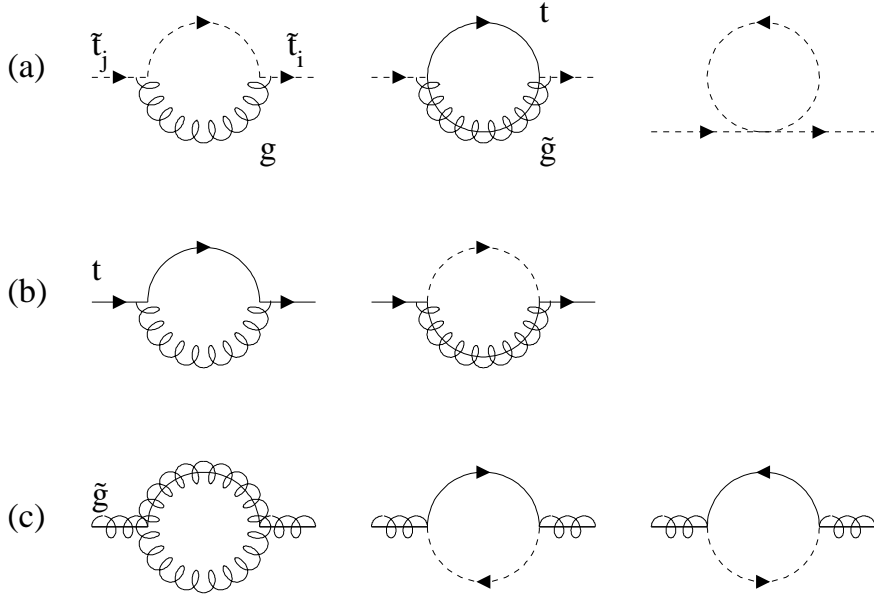


Figure 1: The Feynman diagrams for the self-energies: (a) self-energy of the stop particles, including the mixing due to the second and third diagram; (b) top-quark self-energy; (c) gluino self-energy [including fermion-number violation].

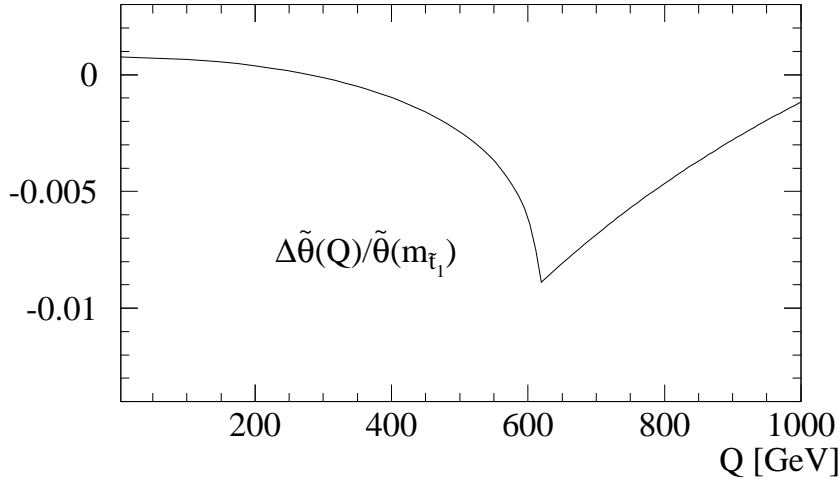


Figure 2: The dependence of $\tilde{\theta}(Q^2)$ on the renormalization scale Q . The normalized shift is shown relative to $\tilde{\theta}(m_{t_1}^2)$: $[\tilde{\theta}(Q^2) - \tilde{\theta}(m_{t_1}^2)]/\tilde{\theta}(m_{t_1}^2)$. The input mass values are the same as for the stop decay to gluinos: $m_{1/2} = 150$ GeV, $m_0 = 800$ GeV, $A_0 = 200$ GeV, $\mu > 0$, for which the leading-order mixing angle is given by 1.24 rad. The minimum of the correction corresponds to the threshold $Q = m_{\tilde{g}} + m_t$ in the scalar integral.

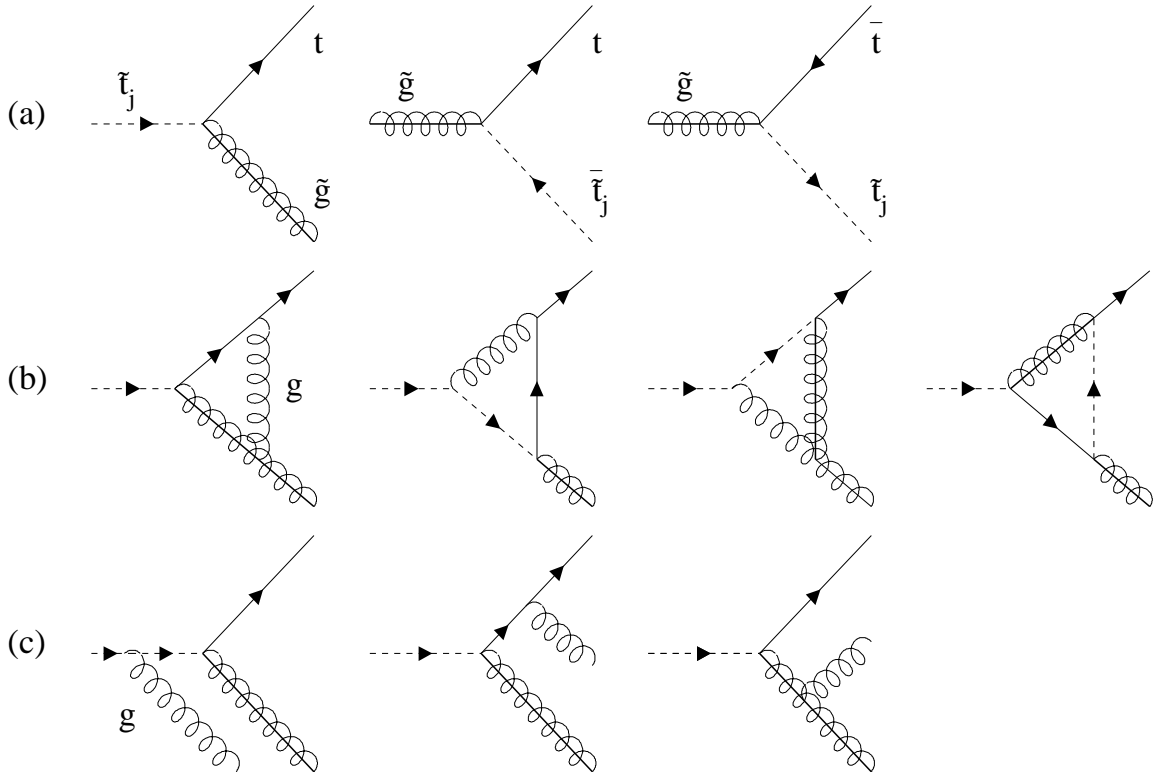


Figure 3: (a) Born diagrams for stop and gluino decays; (b) vertex corrections for stop decays; (c) real-gluon emission for stop decays. The corrections to gluino decays can be obtained by rotating the diagrams.

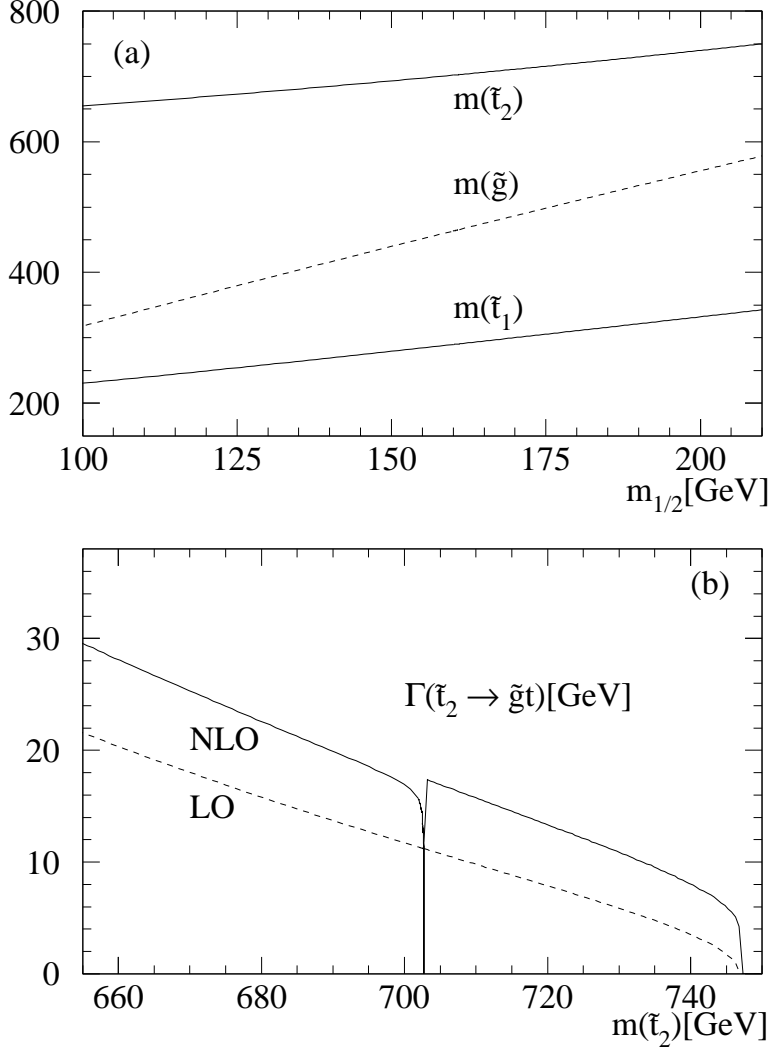


Figure 4: The SUSY-QCD corrections to the decay of heavy stop particles into top quarks and gluinos: (a) the masses of the particles [in GeV] as a function of the common gaugino mass $m_{1/2}$; (b) the decay widths in leading order (dashed curve) and next-to-leading order (solid curve). Input parameter set: $m_0 = 800$ GeV, $A_0 = 200$ GeV, $\mu > 0$. [The kink at the threshold for $\tilde{g} \rightarrow \tilde{t}\bar{t}_1$ can be smoothed out by inserting the finite widths of the particles.]

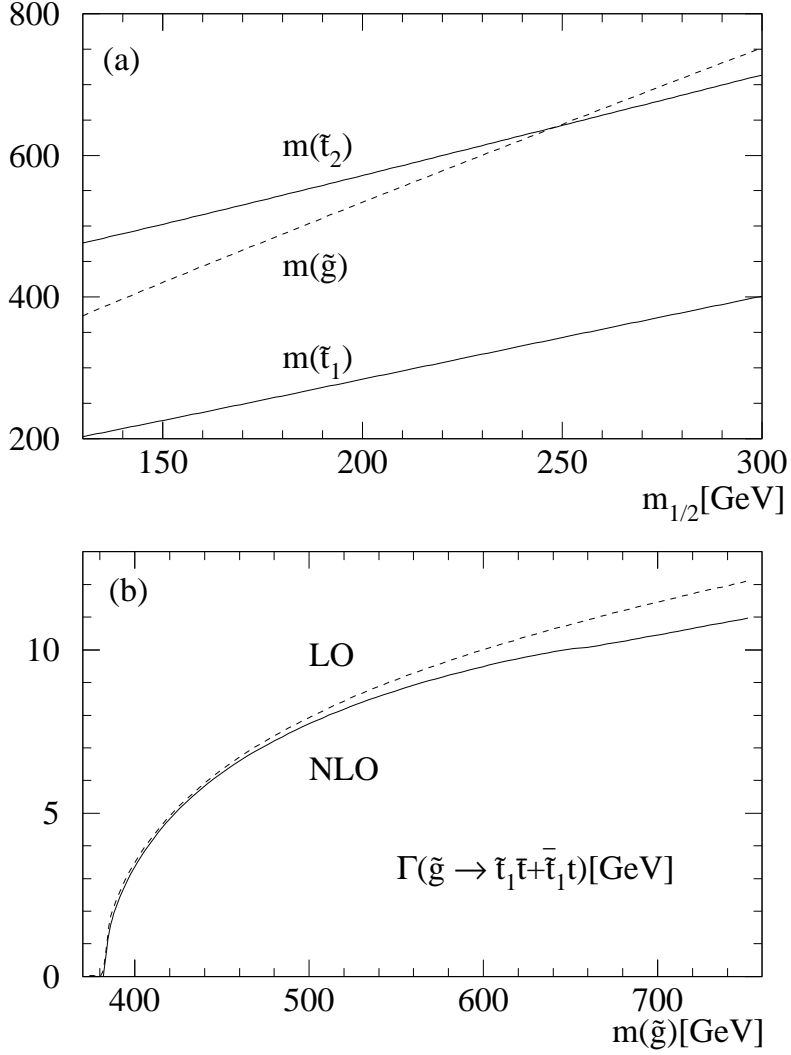


Figure 5: The SUSY-QCD corrections to the decay of gluinos into light stop particles and top quarks: (a) the masses of the particles [in GeV] as a function of the common gaugino mass $m_{1/2}$; (b) the decay widths in leading order (dashed curve) and next-to-leading order (solid curve). Input parameter set: $m_0 = 400$ GeV, $A_0 = 200$ GeV, $\mu > 0$.

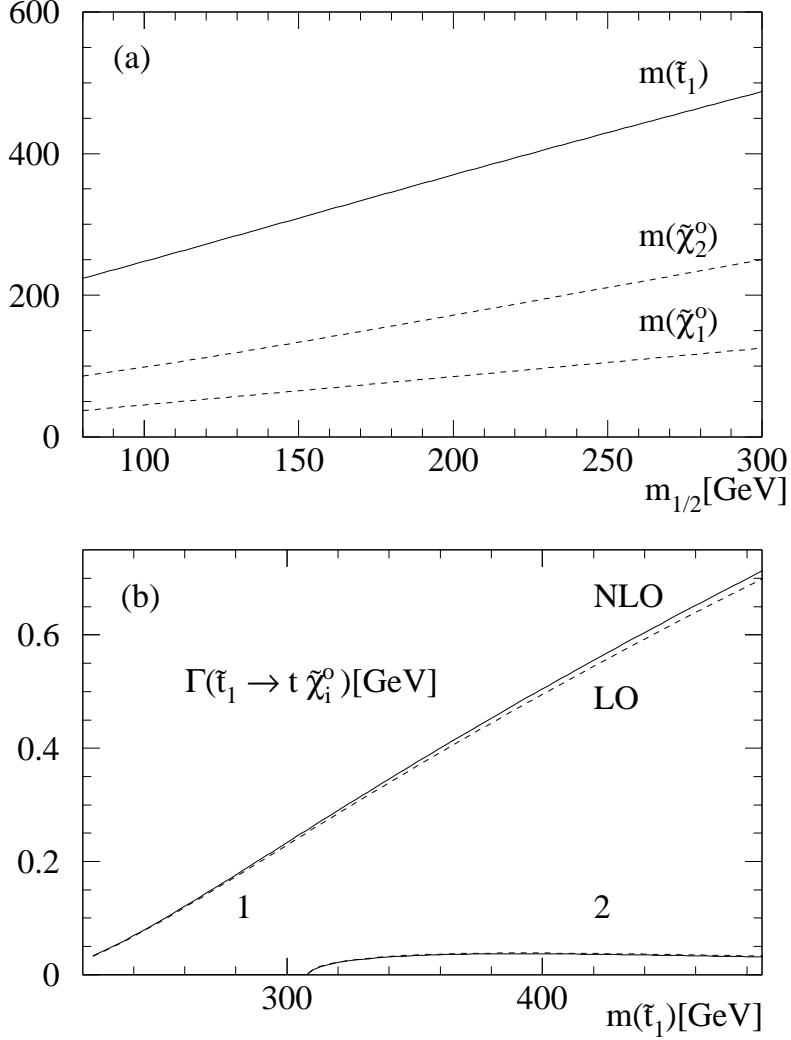


Figure 6: The SUSY-QCD corrections to the decay of light stop particles into top quarks and the possible neutralino eigenstates [see also Ref.[3]]: (a) the masses of the particles [in GeV] as a function of the common gaugino mass $m_{1/2}$; (b) the decay widths in leading order (dashed curve) and next-to-leading order (solid curve). Input parameter set: $m_0 = 50$ GeV, $A_0 = 100$ GeV, $\mu < 0$. Only the decays into the two lightest neutralinos are kinematically allowed for this parameter set.

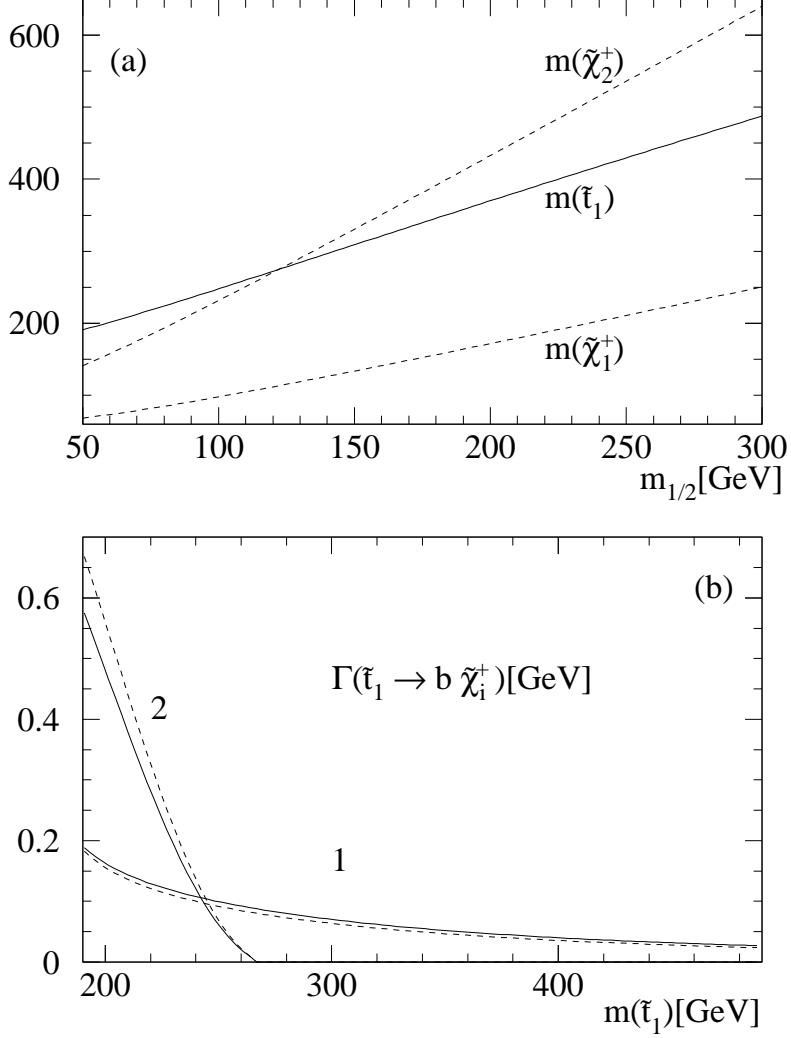


Figure 7: The SUSY-QCD corrections to the decay of light stop particles into bottom quarks and chargino eigenstates [see also Ref.[3]]: (a) the masses of the particles [in GeV] as a function of the common gaugino mass $m_{1/2}$; (b) the decay widths in leading order (dashed curve) and next-to-leading order (solid curve). Input parameter set: $m_0 = 50$ GeV, $A_0 = 100$ GeV, $\mu < 0$.

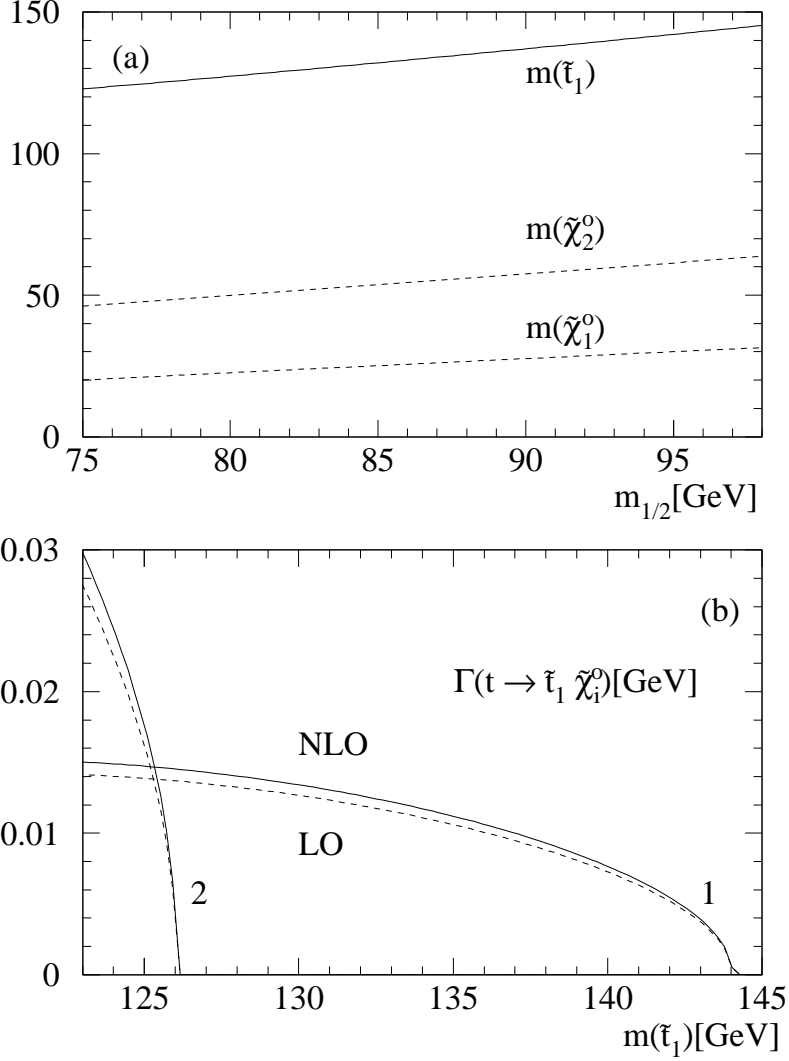


Figure 8: The SUSY-QCD corrections to the decay of top quarks into light \tilde{t}_1 particles and light neutralinos [see also Ref.[5]]: (a) the masses of the particles [in GeV] as a function of the common gaugino mass $m_{1/2}$; (b) the decay widths in leading order (dashed curve) and next-to-leading order (solid curve). Input parameter set: $m_0 = 250$ GeV, $A_0 = 800$ GeV, $\mu > 0$. Only the decays into the two lightest neutralinos are kinematically allowed for this parameter set.